

Rapid Hydrogen–Deuterium Exchange in Liquid Droplets

Erik T. Jansson,^{†,‡,§} Yin-Hung Lai,^{‡,§} Juan G. Santiago,[§] and Richard N. Zare^{*,‡,§}

[†]Department of Chemistry—BMC, Uppsala University, SE-751 24 Uppsala, Sweden

[‡]Department of Chemistry, Stanford University, Stanford, California 94305, United States

[§]Department of Mechanical Engineering, Stanford University, Stanford, California 94305, United States

Supporting Information

ABSTRACT: The rate of hydrogen–deuterium exchange (HDX) in aqueous droplets of phenethylamine has been determined with submillisecond temporal resolution by mass spectrometry using nanoelectrospray ionization with a theta-capillary. The average speed of the microdroplets is measured using microparticle image velocimetry. The droplet travel time is varied from 20 to 320 μs by changing the distance between the emitter and the heated inlet to the mass spectrometer and the voltage applied to the emitter source. The droplets were found to accelerate by $\sim 30\%$ during their observable travel time. Our droplet imaging shows that the theta-capillary produces two Taylor cone–jets (one per channel), causing mixing to take place from droplet fusion in the Taylor spray zone. Phenethylamine ($\phi\text{CH}_2\text{CH}_2\text{NH}_2$) was chosen to study because it has only one functional group ($-\text{NH}_2$) that undergoes rapid HDX. We model the HDX with a system of ordinary differential equations. The rate constant for the formation of $-\text{NH}_2\text{D}^+$ from $-\text{NH}_3^+$ is $3660 \pm 290 \text{ s}^{-1}$, and the rate constant for the formation of $-\text{NHD}_2^+$ from $-\text{NH}_2\text{D}^+$ is $3330 \pm 270 \text{ s}^{-1}$. The observed rates are about 3 times faster than what has been reported for rapidly exchangeable peptide side-chain groups in bulk measurements using stopped-flow kinetics and NMR spectroscopy. We also applied this technique to determine the HDX rates for a small 10-residue peptide, angiotensin I, in aqueous droplets, from which we found a 7-fold acceleration of HDX in the droplet compared to that in bulk solution.

Hydrogen–deuterium exchange (HDX) has been very useful for the study of the dynamics of protein folding and ligand–protein interactions with NMR and mass spectrometry (MS).^{1,2} Understanding how accessible amino acid residues in a protein are to HDX reveals how buried or surface-exposed they are to the surrounding aqueous solution. Typically, only the amide groups in the peptide backbone that slowly exchange hydrogens with D_2O are considered for structural analysis with MS, because the exchange rate of labile hydrogens located in the side chains is about 2 orders of magnitude faster.^{1,3–7} Exposing an amino acid side chain with a primary amine or a hydroxyl group to D_2O causes equilibrium to be reached usually within seconds; by contrast, the amides in the peptide backbone may take several minutes to hours. Therefore, side-chain HDX is very difficult to observe with MS

because the peptides are usually eluted with a liquid chromatography gradient with H_2O in the mobile phase, causing rapid back-exchange. Being able to study the dynamics of HDX in side chains may provide useful complementary structural information. The extremely fast dynamics of peptide side-chain HDX has limited studies to subsecond interactions with MS, in which peptides have been reacted with ND_3 in the gas phase inside the ion transfer system of the MS.^{8–11} Unfortunately, these reactions are far removed from biochemical liquid-phase conditions. We present here a means for determining the liquid-phase rates of HDX in primary amines and peptides with MS. The method is general and may have wide applicability.

We used nanoelectrospray ionization (nanoESI) with a theta-capillary to enable measurements in the liquid phase of rapid HDX in functional groups located in the side chains of peptides. Previously, the Derrick and Williams groups extensively used theta-capillaries for studies of rapid reactions with MS,^{12–16} where different analytes are loaded into each channel and then ejected through nanoESI¹⁷ by applying the same polarity of spray voltage to each channel. The technique can be considered an extension of reactive desorption electrospray ionization (DESI).^{18–20} In addition, experiments in which reactions take place through the fusion of microdroplets have been shown to occur at rates that are up to a million times faster than in bulk.^{19,21–26}

Although there are similarities between the concepts of using theta-capillaries and DESI-spray sources for microdroplet reactions, two major differences are the absence of sheath gas in the nanoESI setup with theta-capillaries and their much smaller tip size. These differences make the resulting droplets much smaller and slower, effectively changing the mixing time of colliding droplets.²⁷ Although measurements of droplet size and velocity have been made for DESI microdroplet reactions, this has never been done for a nanoESI theta-capillary setup, leaving prior estimates of droplet reaction times for theta-capillaries mainly speculative.

Here we found that when using a constant tip size, spray voltage, and backing pressure, the reaction can be modulated by simply moving the theta-capillary back and forth within a range of 0.5–3 mm, as this will change the reaction time during which the reagents interact (during microdroplet collisions), before they enter the mass spectrometer for detection. We loaded the theta-capillary with 1 μM phenethylamine or 1 μM angiotensin

Received: April 8, 2017

Published: May 8, 2017

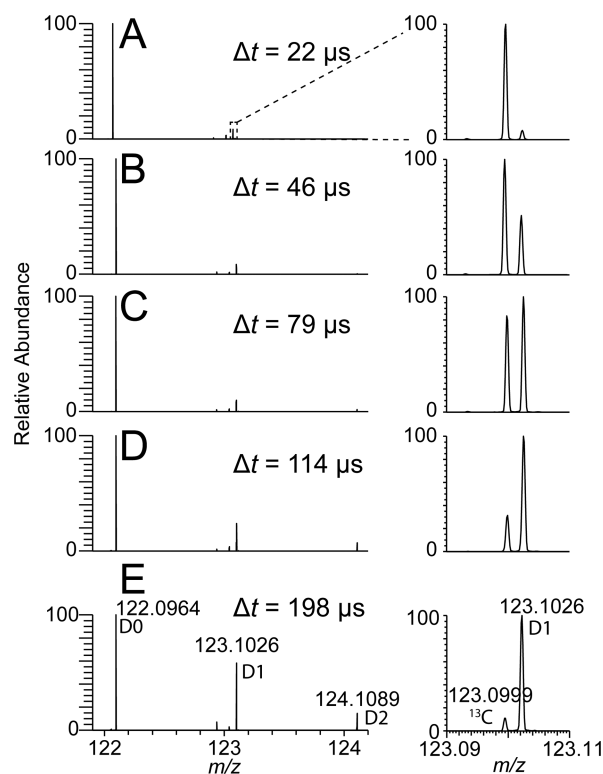


Figure 1. Hydrogen–deuterium exchange observed in phenethylamine m/z 122.096 (D0), with nanoESI using a theta-capillary. The extent of deuteration (D1, m/z 123.103; D2, m/z 124.109) increases by moving the capillary further back from the inlet of the mass spectrometer. (A) $\Delta t = 22 \mu\text{s}$, maximum intensity: 2.4×10^5 ; (B) $\Delta t = 46 \mu\text{s}$, maximum intensity: 3.1×10^5 ; (C) $\Delta t = 79 \mu\text{s}$, maximum intensity: 2.5×10^5 ; (D) $\Delta t = 114 \mu\text{s}$, maximum intensity: 1.4×10^5 ; and (E) $\Delta t = 198 \mu\text{s}$, maximum intensity: 6.4×10^4 ; where Δt is the average dwell time for droplets in air before entering the mass spectrometer. The inset on the right (m/z 123.09–123.11) of each panel shows the relative intensities of the naturally occurring ^{13}C isotope (left) and the D1 isotope (right) of a protonated phenethylamine ion.

I in one channel and D_2O in the other channel to study HDX (Figures 1 and 2).

Phenethylamine is a small aromatic compound (121.2 Da) with a single primary amine; hence, it has two rapidly exchangeable hydrogens (Figure S1A). Angiotensin I is a peptide with 10 amino-acid residues and a monoisotopic mass of 1295.7 Da (Figure S1B). The peptide has 17 groups that have exchangeable hydrogens, out of which 4 are considered to be rapidly exchangeable (primary amines and hydroxyl groups). We monitored HDX of phenethylamine at $[\text{M}+\text{H}]^+$ (Figure 1) and angiotensin I at $[\text{M}+2\text{H}]^{2+}$ (Figure 2). The reaction time is determined by the average time it takes for droplets to mix and travel from the beginning of the mixing zone outside the theta-capillary tip to the MS inlet. We used choline and choline- d_9 as internal standards in each capillary (Figure S2) to monitor the effective mixing rate of analytes reaching the MS. The mixing ratio was found to be $\sim 1:1 \text{ H}_2\text{O}:\text{D}_2\text{O}$. Moving the capillary beyond a 3 mm distance should further increase the reaction time; however we found that at such a distance the signal intensity was too low for analyte detection. We measured the velocity field for microdroplets emitted from a theta-capillary, obtained by imaging the spray with microparticle imaging velocimetry using two Nd:YAG lasers.^{28–30} The droplets were on average $4.3 \mu\text{m}$ in diameter and traveled at average speeds of

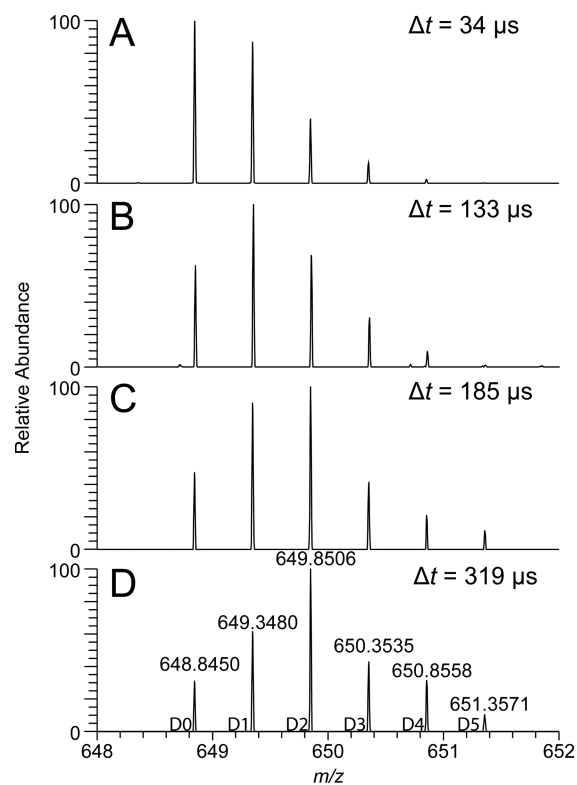


Figure 2. Hydrogen–deuterium exchange observed in angiotensin I, m/z 648.85, with nanoESI using a theta-capillary. The extent of deuteration increases by pulling the capillary further back from the inlet of the mass spectrometer. (A) $\Delta t = 34 \mu\text{s}$, maximum intensity: 2.6×10^6 ; (B) $\Delta t = 133 \mu\text{s}$, maximum intensity: 8.4×10^4 ; (C) $\Delta t = 185 \mu\text{s}$, maximum intensity: 8.0×10^3 ; and (D) $\Delta t = 319 \mu\text{s}$, maximum intensity: 5.6×10^3 ; where Δt is the average dwell time for droplets in air before they enter the mass spectrometer.

$8\text{--}23 \text{ m}\cdot\text{s}^{-1}$ depending on the electric field between the capillary tip ($2.00 \pm 0.18 \mu\text{m}$) and the MS inlet (Table 1, Figures S3–S6, SI Notes 1 and 2).

For phenethylamine, the high mass resolution of the instrument we used allowed us to independently monitor the abundance of the naturally occurring isotopes and the deuterated isotopes as a function of reaction time (Figure 1 and 3A). A decay of the monoisotopic peak was observed for phenethylamine while the deuterated peaks were growing. The deuteration of a compound with n exchangeable hydrogens can be described as a system of coupled reactions with forward and

Table 1. Electric Field Strength E , Average Droplet Velocity u , and Capillary Flow Rates Q during NanoESI as a Function of Distance d and Spray Voltage ϕ When 10 psi N_2 Backing Pressure Was Applied

ϕ (kV)	d (mm)	E ($\text{V}\cdot\text{cm}^{-1}$)	u ($\text{m}\cdot\text{s}^{-1}$)	Q ($\mu\text{L}\cdot\text{min}^{-1}$)
1	0.92	10870	15.3 ± 1.4	1.31 ± 0.24
	1.45	6900	13.6 ± 2.5	1.05 ± 0.19
	1.69	5920	12.7 ± 2.2	0.99 ± 0.18
	2.58	3880	7.8 ± 1.0	0.64 ± 0.11
1.5	0.65	23080	23.3 ± 3.3	1.89 ± 0.34
	1.63	9200	15.2 ± 2.9	1.16 ± 0.21
	1.71	8770	16.0 ± 3.9	1.14 ± 0.21
	1.88	7980	13.6 ± 3.3	0.96 ± 0.17
	2.45	6120	12.8 ± 2.0	1.02 ± 0.18

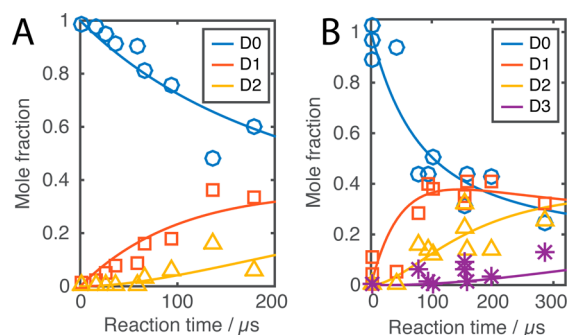
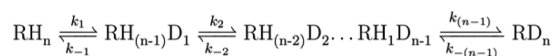


Figure 3. Isotopic patterns resulting from HDX in (A) phenethylamine and (B) angiotensin I (after spectral deconvolution) provided the kinetic behavior of individual components. Labels indicate the monoisotopic peak D0, first deuterated peak D1, second deuterated peak D2, etc. The graphs show the solutions for the systems of ordinary differential equations based on the obtained forward and backward reaction rates. Increasing the distance between the capillary tip and the inlet of the mass spectrometer results in an increased reaction time. As a result, the monoisotopic compound decreases in intensity as HDX proceeds.

Scheme 1. Coupled Reactions of HDX in n States



backward reaction rates k_i and k_{-i} (Scheme 1). We modeled the reaction as a system of ordinary differential equations (SI Note 3) and fitted the rate constants for the observed reactions (Table 2), which were $3660 \pm 290 \text{ s}^{-1}$ for the formation of $-\text{NH}_2\text{D}^+$ from $-\text{NH}_3^+$ and $3330 \pm 270 \text{ s}^{-1}$ for the formation of $-\text{NHD}_2^+$ from $-\text{NH}_2\text{D}^+$, a 3-fold higher rate than what has been observed for primary amines in stopped-flow kinetic experiments performed in bulk.^{1,3–7} For angiotensin I, we observed subsequent shifting of the isotopic envelope to the right (Figure 2). Spectral deconvolution of the data obtained for angiotensin I allowed us to calculate the molar fraction of each component. Figure 3B shows the relative abundance of several isotopes as a function of time. Just like phenethylamine, a decay of the monoisotopic peak was observed for angiotensin I while the deuterated peaks were growing. The first deuterated isotope peak was observed to reach a plateau and then regress, which is expected as HDX of the peptide progresses over time. Table 2 presents the rate constants. For comparison, the decay of the monoisotopic peak for phenethylamine is attributed solely to its primary amine group, but the decay of the monoisotopic peak in angiotensin I is a result of HDX at an ensemble of sites. However, because the exchange rate of the primary amine phenethylamine is ~ 3 times slower than the measured rate of angiotensin I, it is reasonable to consider that HDX in angiotensin I initially happens at hydroxyl groups in the side chain of the peptide. HDX at hydroxyl groups, for example in tyrosine, is 1.5–3 times faster compared to primary amines.^{1,3–7} If the decay rate of angiotensin I is attributed solely

to the tyrosine group that has the fastest exchange rate of all side-chain groups, the lower limit of the rate we observed is 7-fold faster compared to the literature values obtained in bulk reactions, and the ratio between the exchange rate for phenethylamine and angiotensin I in microdroplets appear to be similar to the ratio in bulk.^{1,3–7}

Previous reports suggested that the increased rate observed in microdroplet reactions is a result of evaporation and resulting concentration increase, which in turn would drive the reactions at higher rates.^{19,21} However, in the present study the initial droplet mixing yields a million-fold excess of D_2O in relation to the analyte under study for HDX. We modeled the convective evaporation rate for droplets traveling in air and found that in our system the droplet size is at most decreased by $\sim 1.2\%$ during its flight time (Figure S8, SI Note 4).³¹ This corresponds to a 3.6% reduction of the initial volume. Thus, we can rule out evaporation effects on concentrations and reaction rates. Where does the shift in reaction rates originate? HDX can be acid, base, and/or water catalyzed.^{6,32} Therefore, we hypothesize that the observed changes of rates compared to bulk measurements arise from local pH shifts in the droplets on the surface,^{33,34} caused by a large number of positive charges deposited in the droplets through the ESI mechanism or through concentration redistribution of the positively charged analytes to the surface.^{22,35}

In a nanoESI setup where theta-capillaries are used, the reagents contained in the two channels will not interact until they are ejected from the tip of the theta-capillary. However, no previous studies using a theta-capillary system for nanoESI have attempted to measure the velocity or size of the resulting droplets, such that the effective mixing time has remained unknown. We found two separate Taylor cone–jet regions that repel each other during nanoESI with theta-capillaries (Figure S5, SI Note 1), by imaging the resulting spray at 500 ns intervals with ≤ 25 ns light pulses from Nd:YAG lasers, effectively “freezing” the droplets in each frame. The two channels at the tip orifice are separated by a $0.15 \mu\text{m}$ thick borosilicate wall (a good insulator). A small wetted interface between the two channels should exist; however, we estimate that mixing between the analytes in the Taylor cone–jet region is at least 10^5 times smaller than inertial mixing between droplets colliding with one another in the spray region (Figure S7, SI Note 2). The reaction is expected to be quenched upon entry in the heated capillary as previous studies suggest.^{23,24} Because charged analytes could leave the droplets with no charge left behind on the large droplet through Coulombic fission, our measurements of droplet time of flight should be considered as an upper limit of reaction time. Fission resulting in droplets that are 1 order of magnitude smaller than the parent droplets ($\sim 0.1 \mu\text{m}$) are calculated to evaporate within $30 \mu\text{s}$ and could result in reaction times that are even shorter than what we estimate through the time of flight for the parent droplets. As such, we have here provided a lower limit of the acceleration of reaction rates in microdroplets.

Table 2. Forward and Backward Reaction Rate Constants for Hydrogen–Deuterium Exchange of Phenethylamine and Angiotensin I Calculated for the Experimental Conditions in 50/50 $\text{H}_2\text{O}/\text{D}_2\text{O}$

compound	reaction rate constants (s^{-1})					
	k_1	k_{-1}	k_2	k_{-2}	k_3	k_{-3}
phenethylamine	3660 ± 290	2590 ± 210	3330 ± 270	2350 ± 190		
angiotensin I	9540 ± 760	6750 ± 540	6020 ± 480	4250 ± 340	1086 ± 87	768 ± 61

Chemical reactions in microdroplets are interesting to study because the dispersion of a liquid into droplets shifts the regime from bulk to surface reactions, and the various techniques used are able to characterize reactions down to submillisecond time scales. Also, the apparent rates for many reactions are faster compared to the rates in bulk,^{21–24,26} emphasizing a strong shift of the dynamic behavior of reactions during the transition from bulk to the microscale environment. We suggest that this technique may prove useful for general interrogations of dynamic interactions between ligands and the side chains in a protein.

■ ASSOCIATED CONTENT

Supporting Information

The Supporting Information is available free of charge on the ACS Publications website at DOI: 10.1021/jacs.7b03541.

Materials and methods, Supporting Figures S1–S8, and Supporting Notes 1–4 (PDF)

■ AUTHOR INFORMATION

Corresponding Author

*rnz@stanford.edu

ORCID

Erik T. Jansson: 0000-0002-0675-3412

Yin-Hung Lai: 0000-0003-4245-2016

Juan G. Santiago: 0000-0001-8652-5411

Richard N. Zare: 0000-0001-5266-4253

Notes

The authors declare no competing financial interest.

■ ACKNOWLEDGMENTS

We thank Maria T. Dulay for kind assistance with SEM imaging. E.T.J. was supported by the Swedish Research Council, through award no. 2015-00406. Y.-H. L. was supported by the Program of Talent Development of Academia Sinica, Taiwan. This work has been supported by the National Institute of Mental Health under grant R01-MH112188.

■ REFERENCES

- (1) Englander, S. W.; Kallenbach, N. R. *Q. Rev. Biophys.* **1983**, *16*, 521–655.
- (2) Katta, V.; Chait, B. T. *Rapid Commun. Mass Spectrom.* **1991**, *5*, 214–217.
- (3) Takahashi, T.; Nakanishi, M.; Tsuboi, M. *Bull. Chem. Soc. Jpn.* **1978**, *51*, 1988–1990.
- (4) Takahashi, T.; Nakanishi, M.; Tsuboi, M. *Anal. Biochem.* **1981**, *110*, 242–249.
- (5) Tuchsien, E.; Woodward, C. *Biochemistry* **1987**, *26*, 8073–8078.
- (6) Liepinsh, E.; Otting, G. *Magn. Reson. Med.* **1996**, *35*, 30–42.
- (7) Henry, G. D.; Sykes, B. D. *J. Biomol. NMR* **1995**, *6*, 59–66.
- (8) Rand, K. D.; Pringle, S. D.; Murphy, J. P.; Fadgen, K. E.; Brown, J.; Engen, J. R. *Anal. Chem.* **2009**, *81*, 10019–10028.
- (9) Rand, K. D.; Pringle, S. D.; Morris, M.; Brown, J. M. *Anal. Chem.* **2012**, *84*, 1931–1940.
- (10) Mistarz, U. H.; Brown, J. M.; Haselmann, K. F.; Rand, K. D. *Anal. Chem.* **2014**, *86*, 11868–11876.
- (11) Geller, O.; Lifshitz, C. *J. Phys. Chem. A* **2005**, *109*, 2217–2222.
- (12) Mark, L.; Gill, M.; Mahut, M.; Derrick, P. *Eur. Mass Spectrom.* **2012**, *18*, 439–446.
- (13) Mortensen, D. N.; Williams, E. R. *Anal. Chem.* **2014**, *86*, 9315–9321.
- (14) Mortensen, D. N.; Williams, E. R. *Anal. Chem.* **2015**, *87*, 1281–1287.

(15) Mortensen, D. N.; Williams, E. R. *J. Am. Chem. Soc.* **2016**, *138*, 3453–3460.

(16) Radionova, A.; Greenwood, D. R.; Willmott, G. R.; Derrick, P. J. *Mass Spectrom. Lett.* **2016**, *7*, 21–25.

(17) Wilm, M.; Mann, M. *Anal. Chem.* **1996**, *68*, 1–8.

(18) Song, Y.; Cooks, R. G. *J. Mass Spectrom.* **2007**, *42*, 1086–1092.

(19) Girod, M.; Moyano, E.; Campbell, D. I.; Cooks, R. G. *Chem. Sci.* **2011**, *2*, 501–510.

(20) Perry, R. H.; Splendore, M.; Chien, A.; Davis, N. K.; Zare, R. N. *Angew. Chem., Int. Ed.* **2011**, *50*, 250–254.

(21) Bain, R. M.; Pulliam, C. J.; Cooks, R. G. *Chem. Sci.* **2015**, *6*, 397–401.

(22) Fallah-Araghi, A.; Meguellati, K.; Baret, J.; El Harrak, A.; Mangeat, T.; Karplus, M.; Ladame, S.; Marques, C. M.; Griffiths, A. D. *Phys. Rev. Lett.* **2014**, *112*, 028301.

(23) Müller, T.; Badu-Tawiah, A.; Cooks, R. G. *Angew. Chem., Int. Ed.* **2012**, *51*, 11832–11835.

(24) Lee, J. K.; Kim, S.; Nam, H. G.; Zare, R. N. *Proc. Natl. Acad. Sci. U. S. A.* **2015**, *112*, 3898–3903.

(25) Liu, P.; Zhang, J.; Ferguson, C. N.; Chen, H.; Loo, J. A. *Anal. Chem.* **2013**, *85*, 11966–11972.

(26) Badu-Tawiah, A. K.; Campbell, D. I.; Cooks, R. G. *J. Am. Soc. Mass Spectrom.* **2012**, *23*, 1461–1468.

(27) Carroll, B.; Hidrovo, C. *Heat Transfer Eng.* **2013**, *34*, 120–130.

(28) Meinhart, C. D.; Wereley, S. T.; Santiago, J. G. *J. Fluids Eng.* **2000**, *122*, 285–289.

(29) Meinhart, C.; Wereley, S.; Gray, M. *Meas. Sci. Technol.* **2000**, *11*, 809.

(30) Wereley, S. T.; Meinhart, C. D. *Annu. Rev. Fluid Mech.* **2010**, *42*, 557–576.

(31) Holterman, H. Kinetics and evaporation of water drops in air. IMAG Report 2003-12, Wageningen UR, July 2003.

(32) Jensen, P. F.; Rand, K. D. Hydrogen Exchange: A Sensitive Analytical Window into Protein Conformation and Dynamics. In *Hydrogen Exchange Mass Spectrometry of Proteins*; John Wiley & Sons, Ltd.: New York, 2016; pp 1–17.

(33) Zhou, S.; Prebyl, B. S.; Cook, K. D. *Anal. Chem.* **2002**, *74*, 4885–4888.

(34) Girod, M.; Dagany, X.; Antoine, R.; Dugourd, P. *Int. J. Mass Spectrom.* **2011**, *308*, 41–48.

(35) Li, Y.; Yan, X.; Cooks, R. G. *Angew. Chem., Int. Ed.* **2016**, *55*, 3433–3437.